



1 **History of anthropogenic Nitrogen inputs (HaNi) to the terrestrial biosphere:**  
2 **A 5-arcmin resolution annual dataset from 1860 to 2019**

3 Hanqin Tian<sup>1\*</sup>, Zihao Bian<sup>1\*</sup>, Hao Shi<sup>2,1\*</sup>, Xiaoyu Qin<sup>2</sup>, Naiqing Pan<sup>1</sup>, Chaoqun Lu<sup>3</sup>, Shufen  
4 Pan<sup>1</sup>, Francesco N. Tubiello<sup>4</sup>, Jinfeng Chang<sup>5</sup>, Giulia Conchedda<sup>4</sup>, Junguo Liu<sup>6</sup>, Nathaniel  
5 Mueller<sup>7,8</sup>, Kazuya Nishina<sup>9</sup>, Rongting Xu<sup>10</sup>, Jia Yang<sup>11</sup>, Liangzhi You<sup>12</sup>, Bowen Zhang<sup>13</sup>

6  
7 <sup>1</sup>International Center for Climate and Global Change Research and School of Forestry and  
8 Wildlife Sciences, Auburn University, Auburn, AL 36849, USA; <sup>2</sup>Research Center for Eco-  
9 Environmental Sciences, State Key Laboratory of Urban and Regional Ecology, Chinese  
10 Academy of Sciences, Beijing 100085, China; <sup>3</sup>Department of Ecology, Evolution, and  
11 Organismal Biology, Iowa State University, Ames, IA 50011, USA; <sup>4</sup>Statistics Division, Food  
12 and Agriculture Organization of the United Nations, Via Terme di Caracalla, Rome, Italy;  
13 <sup>5</sup>College of Environmental and Resource Sciences, Zhejiang University, Hangzhou 310058,  
14 China; <sup>6</sup>School of Environmental Science and Engineering, Southern University of Science and  
15 Technology, Shenzhen 518055, China. <sup>7</sup>Department of Ecosystem Science and Sustainability,  
16 Colorado State University, Fort Collins, CO 80523, USA; <sup>8</sup>Department of Soil and Crop  
17 Sciences, Colorado State University, Fort Collins, CO 80523, USA; <sup>9</sup>Biogeochemical Cycle  
18 Modeling and Analysis Section, Earth System Division, National Institute for Environmental  
19 Studies 16-2, Onogawa, Tsukuba, 305-8506, JAPAN; <sup>10</sup>Forest Ecosystems and Society, Oregon  
20 State University, Corvallis, OR 97330, USA; <sup>11</sup>Department of Natural Resource Ecology and  
21 Management, Oklahoma State University, Stillwater, OK 74078, USA; <sup>12</sup>International Food  
22 Policy Research Institute (IFPRI), 1201 Eye Street, NW, Washington, DC 20005, USA;  
23 <sup>13</sup>Department of Environment, Geology, and Natural Resources, Ball State University, Muncie,  
24 IN 47306, USA

25  
26

*\*Corresponding authors:*

Hanqin Tian ([tianhan@auburn.edu](mailto:tianhan@auburn.edu));

Zihao Bian ([zzb0009@auburn.edu](mailto:zzb0009@auburn.edu));

Hao Shi ([haoshi@rcees.ac.cn](mailto:haoshi@rcees.ac.cn))

27



## 28 Abstract

29 Excessive anthropogenic nitrogen (N) inputs to the biosphere have disrupted the global nitrogen  
30 cycle. To better quantify the spatial and temporal patterns of anthropogenic N enrichments, assess  
31 their impacts on the biogeochemical cycles of the planet and other living organisms, and improve  
32 nitrogen use efficiency (NUE) for sustainable development, we have developed a comprehensive  
33 and synthetic dataset for reconstructing the History of anthropogenic N inputs (HaNi) to the  
34 terrestrial biosphere. The HaNi dataset takes advantage of different data sources in a  
35 spatiotemporally consistent way to generate a set of high-resolution gridded N input products from  
36 the preindustrial to present (1860-2019). The HaNi dataset includes annual rates of synthetic N  
37 fertilizer, manure application/deposition, and atmospheric N deposition in cropland, pasture, and  
38 rangeland at a spatial resolution of 5-arcmin. Specifically, the N inputs are categorized, according  
39 to the N forms and land uses, as ten types: 1)  $\text{NH}_4^+$ -N fertilizer applied to cropland, 2)  $\text{NO}_3$ -N  
40 fertilizer applied to cropland, 3)  $\text{NH}_4^+$ -N fertilizer applied to pasture, 4)  $\text{NO}_3$ -N fertilizer applied  
41 to pasture, 5) manure N application on cropland, 6) manure N application on pasture, 7) manure  
42 N deposition on pasture, 8) manure N deposition on rangeland, 9)  $\text{NH}_x$ -N deposition, and 10)  $\text{NO}_y$ -  
43 N deposition. The total anthropogenic N (TN) inputs to global terrestrial ecosystems increased  
44 from 29.05 Tg N  $\text{yr}^{-1}$  in the 1860s to 267.23 Tg N  $\text{yr}^{-1}$  in the 2010s, with the dominant N source  
45 changing from atmospheric N deposition (before the 1900s) to manure N (the 1910s-2000s), and  
46 to synthetic fertilizer in the 2010s. The proportion of synthetic  $\text{NH}_4^+$ -N fertilizer increased from  
47 64% in the 1960s to 90% in the 2010s, while synthetic  $\text{NO}_3$ -N fertilizer decreased from 36% in  
48 the 1960s to 10% in the 2010s. Hotspots of TN inputs shifted from Europe and North America to  
49 East and South Asia during the 1960s-2010s. Such spatial and temporal dynamics captured by the  
50 HaNi dataset are expected to facilitate a comprehensive assessment of the coupled human-earth  
51 system and address a variety of social welfare issues, such as climate-biosphere feedback, air  
52 pollution, water quality, and biodiversity.

53

54



## 55 1. Introduction

56 Nitrogen (N) is an essential element for the survival of all living organisms, required by various  
57 biological molecules, for instance, nucleic acids, proteins, and chlorophyll (Galloway et al., 2021;  
58 Schlesinger and Bernhardt, 2020). Most N on the Earth is not readily available for organisms, since  
59 it either exists in the form of inert N<sub>2</sub> gas or is stored in crust and sediments (Ward, 2012). Driven  
60 by the human demand for food and energy, a spectrum of approaches have been developed to  
61 produce biologically available N (Sutton et al., 2013; Lassaletta et al. 2016), ranging from traditional  
62 methods, such as legume crops cultivation and manure application, to modern techniques, such as  
63 industrial compost and the Haber-Bosch process that produce organic fertilizer mixture and  
64 chemical fertilizer. Increasing anthropogenic N inputs have significantly boosted crop yield and  
65 improved food security (Stewart and Roberts, 2012), but also resulted in over twofold increase in  
66 terrestrial reactive N (Galloway and Cowling 2002; Fowler et al. 2013; Melillo, 2021; Scheer et  
67 al., 2020) and are expected to continually increase in the coming decades due to human demand  
68 for food (Kanter et al. 2020; Sutton et al. 2021).

69 The large amount of excessive reactive N in terrestrial ecosystems has led to multiple  
70 environmental issues like water quality deterioration, air pollution, global warming, and  
71 biodiversity loss (Bouwman et al., 2005; Gruber and Galloway, 2008; Howarth, 2008; Pan et al.,  
72 2021; Tian et al., 2020a; Vitousek et al., 1997). The river export of various forms of nitrogen  
73 (ammonium, nitrate, dissolved organic N) has largely increased (Schlesinger et al., 2006; Tian et  
74 al., 2020b), frequently causing large-scale hypoxia along coastal oceans for example, in the  
75 northern Gulf of Mexico (Bargu et al., 2019; Dodds, 2006; Rabalais and Turner, 2019). The global  
76 emission of ammonia (NH<sub>3</sub>), a toxic pollutant and a major precursor of aerosol, had rapidly  
77 increased from 1.0 Tg N yr<sup>-1</sup> in 1961 to 9.9 Tg yr<sup>-1</sup> in 2010, mainly due to the wide use of N  
78 fertilizer (Xu et al., 2019a). The emissions of nitrous oxide (N<sub>2</sub>O), the third most important  
79 greenhouse gas, had increased by 30% over the past four decades, which was mainly attributed to  
80 N addition to croplands (Cui et al., 2021; Tian et al., 2020a). Moreover, excessive usage of N over  
81 other nutrients (e.g. phosphorus) brings nutrient imbalance that may induce significant alterations  
82 in the structure and functions of ecosystems and finally result in losses of biodiversity (Galloway  
83 et al., 2003; Lun et al., 2018; Peñuelas and Sardans, 2022; Houlton et al., 2019).



84 In light of the critical impacts of N excess on the human-earth system, numerous efforts have been  
85 conducted to generate distribution maps of N inputs for different sectors with varied temporal  
86 coverage and spatial resolution (Potter et al., 2010; Nishina et al., 2017; Bian et al., 2021; Liu et  
87 al., 2010). Country-level N fertilizer data from the Food and Agriculture Organization of the  
88 United Nations (FAO) and the International Fertilizer Association (IFA) have been widely used to  
89 assess global and national nitrogen budgets for crop production (Xiong et al., 2008; Zhang et al.,  
90 2021; Eickhout et al., 2006). However, spatial variations of N inputs within countries have been  
91 overlooked in country-level data, while detailed geospatial distributions of N inputs are required  
92 for many process-based modeling studies (Tian et al., 2019, 2018). Potter et al. (2010) and Mueller  
93 et al. (2012) both generated crop-specific spatially-explicit N fertilizer data which, however,  
94 represented the average fertilizer application patterns around 2000. Liu et al. (2010) developed a  
95 N balance model, and made the first attempt to quantify six N inputs (e.g. mineral fertilizer, manure,  
96 atmospheric deposition, biological fixation, input from sedimentation, and input from recycled  
97 crop residual) and five N outputs (e.g. output to harvested crops, crop residues, leaching, gaseous  
98 losses, and soil erosion) in cropland for the year 2000 with a spatial resolution of 5-arcmin. Lu and  
99 Tian (2017) created an annual dataset of global N fertilizer application in cropland at a spatial  
100 resolution of  $0.5^\circ \times 0.5^\circ$  during 1961-2013, and Nishina et al. (2017) further split synthetic N  
101 fertilizer application into  $\text{NH}_4^+$  and  $\text{NO}_3^-$  forms. Meanwhile, Zhang et al. (2017) reconstructed  
102 global manure N production and application rates in cropland which covered the period 1860-2014  
103 and had a resolution of 5-arcmin; using a similar methodology, Xu et al., (2019b) further developed  
104 three gridded datasets, i.e., rangeland manure deposition, pasture manure deposition, and pasture  
105 manure application, all of which had a resolution of  $0.5^\circ \times 0.5^\circ$  and spanned from 1860-2016.  
106 Although these datasets are valuable in addressing their respective objective issues, there is a  
107 barrier in taking advantage of them simultaneously, due to the inconsistent temporal coverage,  
108 spatial resolution, data sources (e.g., N inputs statistics and land use), and spatial allocation  
109 algorithms. Therefore, the reconstruction for the History of Anthropogenic N Inputs (HaNi) to the  
110 terrestrial biosphere with rich spatial details and long-term coverage is essentially needed.

111 To address this issue, using sophisticated methodologies, we employed multiple statistical data,  
112 empirical estimates, atmospheric chemistry model outputs (Eyring et al., 2013), and high-  
113 resolution land-use products to generate the HaNi dataset. This comprehensive dataset consists of  
114 N fertilizer/manure application to cropland, manure application/deposition to pasture, manure



115 deposition to rangeland, and atmospheric N deposition on all agricultural land at a resolution of 5-  
116 arcmin from 1860 to 2019. Additionally, we tried to investigate the impacts of social-economic  
117 forcing on N use across different regions. These efforts are anticipated to benefit understanding  
118 the spatial and temporal patterns of human-induced N enrichment, assessing impacts of excessive  
119 N on global and regional biogeochemical cycles, and providing data support for resource  
120 management. The HaNi dataset has also been expected to serve as input data for Earth system  
121 models, biogeochemical models, and hydrological models for improving our understanding and  
122 assessment of global consequences of anthropogenic nitrogen enrichment for climate change, air  
123 and water quality, ecosystems, and biodiversity (e.g. Tian et al., 2018).

## 124 **2. Methods**

### 125 **2.1. Data sources of fertilizer/manure use**

126 Multiple anthropogenic N input databases were integrated to generate the HaNi dataset (Table 1).  
127 For the period of 1961-2019, annual country-level statistics data was obtained from the FAOSTAT  
128 “Land, Inputs and Sustainability” domain (FAO, 2021). “N fertilizer applied to soil” was from the  
129 “Fertilizers by Nutrient” subsection. “Manure applied to soil” and “Manure left on pasture” data  
130 were from the “Livestock Manure” subsection. Before 1961, the time series of fertilizer and  
131 manure use from Holland et al. (2005) was adopted and corrected to be consistent with FAO  
132 statistics. For countries (e.g., the former Soviet Union, the Socialist Federal Republic of  
133 Yugoslavia, Eritrea, Ethiopia, and the Czechoslovak Republic) that experienced political  
134 disintegration, we partitioned their pre-disintegration N fertilizer/manure use into each individual  
135 new-formed country using the ratios derived from the N uses of the new-formed countries in the  
136 first year after disintegration.

137 The FAOSTAT agricultural use of N fertilizer and manure referred to the N use for crops, livestock,  
138 forestry, fisheries, and aquaculture, excluding N use for animal feed. Since the use of N fertilizers  
139 and manure for forestry, fisheries, and aquaculture was minor compared to that for crops and  
140 livestock, this part was taken as neglectable. The partitioning ratio of N fertilizer application to  
141 cropland and pasture was adopted from Lassaletta et al. (2014). Since Lassaletta’s ratio values only  
142 covered the period of 1961-2009, values in 2009 were used to calculate the N application  
143 partitioning after 2009. By FAO’s definition, manure applied to soil was equal to the difference  
144 between all treated manure and N loss during stored and treated processes. Therefore, we assumed



145 that the total quantity of manure applied to soil was equal to the total quantity of manure applied  
146 to cropland and pasture. The fraction values for cropland were from Zhang et al. (2015), who  
147 assumed the fraction value ranged between 0.5 and 0.87 for European countries, Canada, and the  
148 U.S., while it was 0.9 for other countries.

## 149 **2.2 Land use data**

150 The HYDE3.2 dataset (Klein Goldewijk et al., 2017) provides historical spatial distributions of  
151 cropland, pasture, and rangeland at a 5-arcmin resolution and at an annual time-step after 2000 but  
152 a decadal time-step before the 1990s. In contrast, the LUHv2 dataset (Hurt et al., 2020), derived  
153 mainly from HYDE3.2, has an annual time-step across 1860-2019 but at a relatively low spatial  
154 resolution of  $0.25^\circ \times 0.25^\circ$ . To reconcile these two datasets, we first conducted a linear  
155 interpolation to HYDE3.2 before 1999 using the data of every two neighbor decades. Then the  
156 fraction of crop/pasture/rangeland of a LUHv2 grid was partitioned into all grid cells of HYDE3.2  
157 that fell in the LUHv2 grid, according to their shares in HYDE3.2. Through this routine, we  
158 obtained a land-use dataset that both kept spatial information of HYDE3.2 and was consistent with  
159 LUHv2 on the total area for each land use type.

## 160 **2.3 Spatializing N fertilizer and manure application in cropland**

161 The workflow of spatializing the country-level N fertilizer and manure use amount to gridded maps  
162 is shown in Fig 1. First, the grid-level crop-specific N fertilizer and manure use rates per cropland  
163 area of 17 dominant crop types (wheat, maize, rice, barley, millet, sorghum, soybean, sunflower,  
164 potato, cassava, sugarcane, sugar beet, oil palm, rapeseed, groundnut, cotton, and rye), which were  
165 developed by Mueller et al. (2012) and West et al. (2014), were combined with the crop-specific  
166 harvested area (Monfreda et al. 2008) to generate baseline distribution maps circa 2000 of fertilizer  
167 and manure application in cropland. The crop-area-based average N fertilizer and manure rates in  
168 each grid cell (at a resolution of 5-arcmin) were calculated as:

$$169 \quad \overline{C_{fer/man}} = \frac{\sum_i (C_{fer/man,i} \times AH_i)}{\sum_i AH_i} \quad (1)$$

170 where  $\overline{C_{fer/man}}$  is the area-weighted average of N fertilizer or manure application rates (i.e.,  
171 gridded baseline fertilizer or manure application rate, in the unit of  $\text{g N m}^{-2} \text{cropland yr}^{-1}$ ).  
172  $C_{fer/man,i}$  and  $AH_i$  are crop-specific N fertilizer or manure application rate ( $\text{g N m}^{-2}$ ) and  
173 harvested area ( $\text{m}^2$ ), respectively, for crop type  $i$ .



174 Second, we used annual country-level N fertilizer and manure application amounts from FAO  
175 (1961-2019) and the annual cropland area to scale the baseline year 2000 maps of N fertilizer and  
176 manure application rates across time using the following equation:

$$177 \quad R_{fer/man,y,j} = \frac{FAO_{fer/man,y,j}}{\sum_{g=1}^{g=n \text{ in country } j} (\overline{C_{fer/man}} \times AC_{y,g})} \quad (2)$$

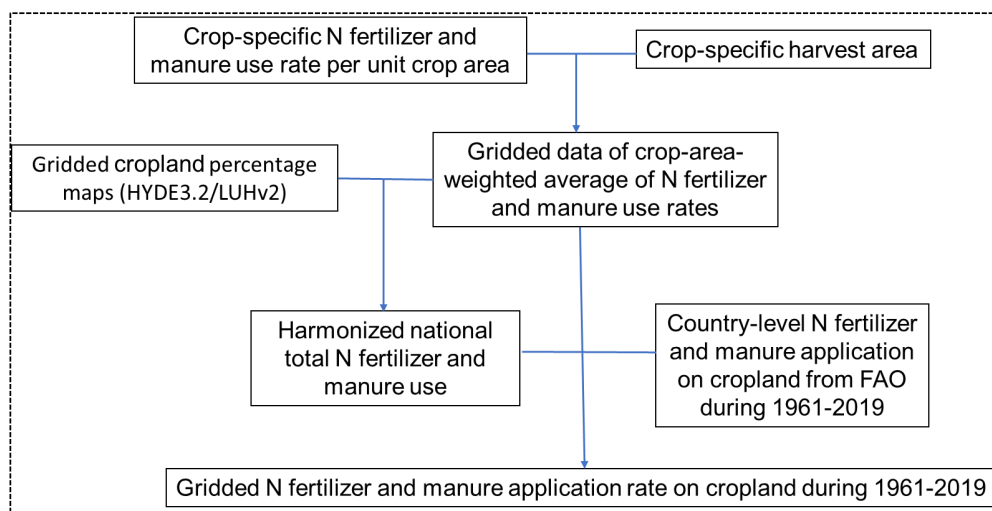
178 where  $R_{fer/man,y,j}$  is the regulation ratio (unitless) in the year  $y$  and country  $j$ .  $FAO_{fer/man,y,j}$  is  
179 country-level total N fertilizer or manure use amount ( $\text{g N yr}^{-1}$ ) on cropland derived from  
180 FAOSTAT.  $AC_{y,g}$  is the area of cropland ( $\text{m}^2$ ) derived from the historical land use data in the year  
181  $y$  and grid  $g$ . The actual N fertilizer and manure application rates were then calculated using the  
182 following equation:

$$183 \quad N_{fer/man} = \overline{C_{fer/man}} \times R_{fer/man,y} \quad (3)$$

184 where  $N_{fer/man}$  is the “real” gridded N fertilizer or manure use rates ( $\text{g N m}^{-2} \text{cropland yr}^{-1}$ ) in  
185 the year  $y$ .

186 Then, we extended the fertilizer data back to 1925 and manure data back to 1860 using the global  
187 N flux change rates (Holland et al. 2005). Since industrial production of synthetic fertilizer was  
188 developed in the early 1910s, we further extend fertilizer data back by assuming the fertilizer  
189 production linearly increased from 1910 to 1925. Finally, N fertilizer application in cropland was  
190 further divided into the  $\text{NH}_4^+$  form the  $\text{NO}_3^-$  form based on the annual country-level  $\text{NH}_4^+$   
191 application ratio in total N fertilizer provided by Nishina et al. (2017). This data was estimated  
192 based on FAOSTAT's consumption data by chemical fertilizer type, which takes into account the  
193  $\text{NH}_4^+$  and  $\text{NO}_3^-$  content in each fertilizer type individually.

194



195

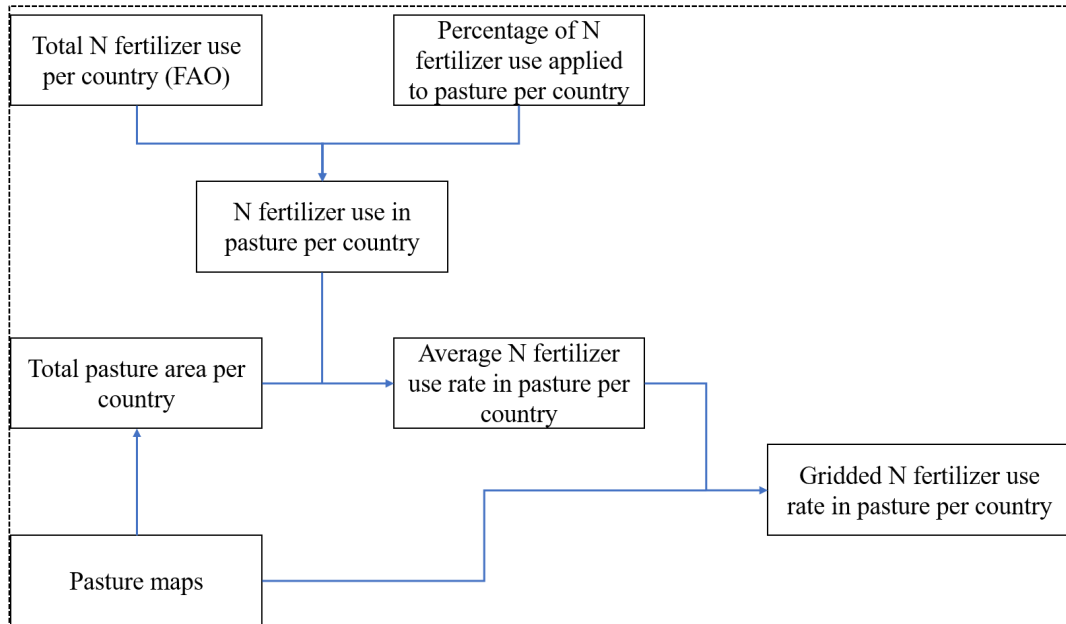
196 **Figure 1.** The workflow for developing the dataset of global annual N fertilizer and manure  
197 application rates during 1961-2019.

198

## 199 **2.4. Spatializing the total manure N in pasture and rangeland**

### 200 **2.4.1. N fertilizer use in pasture**

201 Due to the lack of grid-level spatial information of N fertilizer use in pasture, we assumed that  
202 pasture within each country has an even annual N fertilizer use rate. The fertilizer use in pasture  
203 per country was divided by the total pasture area of that country. Then this N fertilizer use rate per  
204 country was assigned to all the pasture grid cells in that country (Fig 2). The detailed method was  
205 introduced in Xu et al. (2019b).



206

207 **Figure 2.** The workflow for developing the global pasture fertilizer application rate data during  
 208 1961-2019.

#### 209 2.4.2. Spatializing manure application in pasture

210 To generate spatial patterns of manure application in pasture, we first calculated the spatial  
 211 distribution of annual manure N production. The Global Livestock of World 3 database (GLW3;  
 212 Gilbert et al., 2018) was used as a reference map of livestock distribution, which provided spatial  
 213 information for buffaloes, cattle, chickens, ducks, horses, goats, pigs, and sheep at a spatial  
 214 resolution of  $0.083^\circ$  in 2010. For the period 1961-2019, the FAO statistics of livestock population  
 215 in a country in one year was compared with the sum of GLW3 grid values within that country and  
 216 the ratio of the two values was used to scale all the GLW3 grid values of the country to generate  
 217 the spatial distribution of livestock in that year (Fig. 3). This routine can be represented as:

$$218 \quad D_{l,c,y}^{FAO} = D_{l,c}^{GLW3} \times \frac{T_{l,c,y}^{FAO}}{T_{l,c}^{GLW3}} \quad (4)$$

219 where  $T_{l,c,y}^{FAO}$  indicates the FAO statistics of the population of the  $l$ th type of livestock of country  $c$   
 220 in year  $y$ ,  $T_{l,c}^{GLW3}$  indicates the national population of the  $l$ th type of livestock of country  $c$   
 221 summarized from GLW3,  $D_{l,c}^{GLW3}$  is the spatial distribution corresponding to  $T_{l,c}^{GLW3}$ , and  $D_{l,c,y}^{FAO}$  is



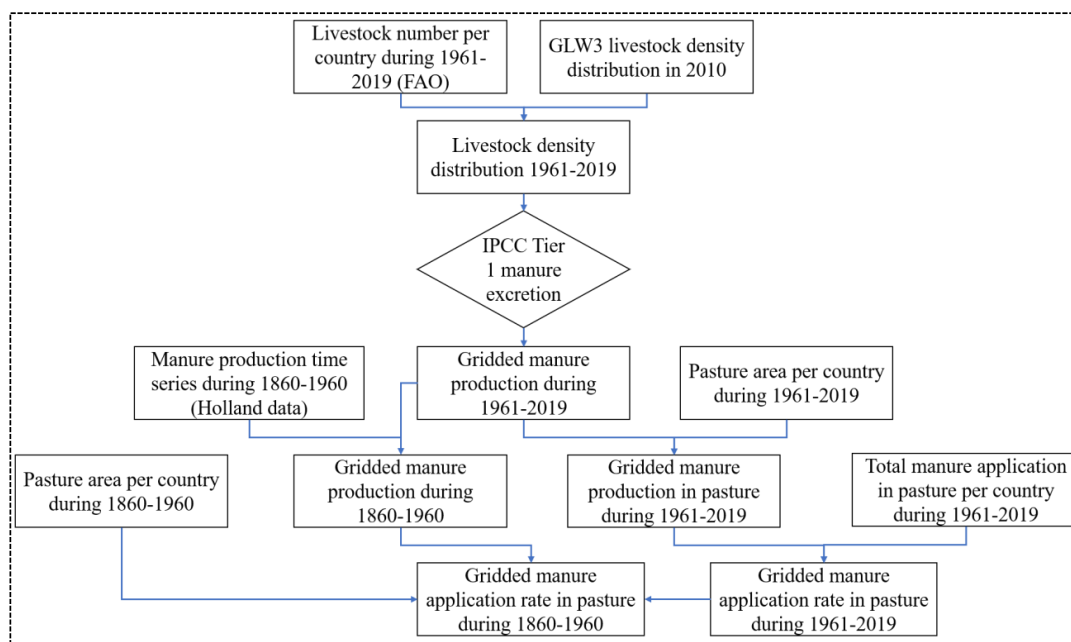
222 the corresponding spatial distribution to  $T_{l,c,y}^{FAO}$ . Applying the IPCC Tier 1 methodology for N  
223 excretion (Dong et al., 2006) to these derived spatial distribution maps of livestock, we can have  
224 the spatial maps of annual manure production during 1961-2019. Specifically, the average daily N  
225 excretion rate was different for each livestock and for each group of countries, which were  
226 classified by socioeconomic and geographic conditions. All manure production data were  
227 resampled to 5-arcmin to be consistent with the pasture land use data.

228 Manure application to pasture during 1961-2019 is then estimated using manure production and  
229 pasture area (Fig. 3) as:

$$230 \quad R_{c,y}^{Nprod/Napp} = \frac{\text{sum}(GNprod_{c,y}^{FAO} \times GParea_{c,y}^{LU})}{Napp_{c,y}^{FAO}} \quad (5)$$

$$231 \quad GNapp_{c,y}^{FAO} = \text{mask}(R_{c,y}^{Nprod/Napp} \times GNprod_{c,y}^{FAO}, GParea_{c,y}^{LU}) \quad (6)$$

232 where  $R_{c,y}^{Nprod/Napp}$  is the ratio of N production over FAO manure application to pasture in  
233 country  $c$  in year  $y$ ,  $GNprod_{c,y}^{FAO}$  is the gridded manure production in country  $c$  in year  $y$  estimated  
234 based on FAO statistics of livestock data,  $GParea_{c,y}^{LU}$  is the gridded pasture area in country  $c$  in  
235 year  $y$  from our land use data, and  $GNapp_{c,y}^{FAO}$  is the corresponding gridded manure application to  
236 pasture in country  $c$  in year  $y$  through masking the product raster of  $R_{c,y}^{Nprod/Napp}$  and  $GNprod_{c,y}^{FAO}$   
237 by the  $GParea_{c,y}^{LU}$  raster. The manure application to pasture in year  $y$  during 1860-1960 was  
238 estimated as the product of  $GNprod_{c,y}^{Holland}$  and  $R_{c,1961}^{Nprod/Napp}$  (Fig 3). As for the period 1860-1960,  
239 the time series of manure application data were also generated according to the manure N change  
240 rates derived from Holland et al. (2005).



241

242 **Figure 3.** The workflow for developing the global pasture manure application rate data during  
243 1860-2019.

244

### 245 2.4.3. Spatializing manure deposition in pasture and rangeland

246 The routine for spatializing FAO statistics of manure deposition on pasture and rangeland was  
247 similar to the method for manure application to pasture in Xu et al. (2019b). The only difference  
248 is that the manure deposition intensity on pasture was assumed to be twice that on rangeland within  
249 a grid cell, according to previous research (Campbell and Stafford Smith, 2000).

### 250 2.5 Atmospheric nitrogen deposition

251 Monthly atmospheric N depositions (NH<sub>x</sub>-N and NO<sub>y</sub>-N) during 1850–2014 were from N  
252 deposition fields of model simulations in the International Global Atmospheric Chemistry  
253 (IGAC)/Stratospheric Processes and Their Role in Climate (SPARC) Chemistry–Climate Model  
254 Initiative (CCMI) (Morgenstern et al., 2017). For the period 2015-2020, N deposition under  
255 SSP585 was used, consistent with TRENDY simulations for the global carbon budget  
256 (Friedlingstein et al., 2020). The CCMI models considered N emissions from multiple sources,  
257 including anthropogenic and biofuel sources, natural biogenic sources, biomass burning and  
258 lightning, and the transport of N gases and wet/dry N deposition (Eyring et al., 2013). The CCMI



259 N deposition data was developed in support of the Coupled Model Intercomparison Project Phase  
 260 6 (CMIP6) and used as the official products for CMIP6 models that lack interactive chemistry  
 261 components. The nearest interpolation method was used to resample N deposition data to a spatial  
 262 resolution of 5-arcmin.

## 263 **2.6 Regional Analysis**

264 In order to compare anthropogenic N inputs across different regions, we divided the global land  
 265 area into 18 regions according to national or continental boundaries (Tian et al. 2019). The 18  
 266 regions are USA, Canada (CAN), Central America (CAM), Northern South America (NSA),  
 267 Brazil (BRA), Southwest South America (SSA), Europe (EU), Northern Africa (NAF), Equatorial  
 268 Africa (EQUAF), Southern Africa (SAF), Russia (RUS), Central Asia (CAS), Middle East (MIDE),  
 269 China (CHN), Korea and Japan (KAJ), South Asia (SAS), Southeast Asia (SEAS), and Oceania  
 270 (OCE).

## 271 **3. Results**

### 272 **3.1. Temporal and spatial changes in total anthropogenic N inputs**

273 The total anthropogenic N (TN) inputs to global terrestrial ecosystems increased from 29.05 Tg N  
 274 yr<sup>-1</sup> in the 1860s to 267.23 Tg N yr<sup>-1</sup> in the 2010s (Fig 4 and Table 2). The most rapid increase of  
 275 total N inputs was 3.53 Tg N yr<sup>-2</sup> occurred during 1945-1990 driven by both elevated fertilizer  
 276 application rates and cropland expansion. The TN inputs leveled off within the 1990s, but  
 277 increased again after 2001 with a lower increasing rate though. The TN inputs were dominated by  
 278 atmospheric N deposition before the 1900s. Manure N kept an increasing trend, accounting for  
 279 more than half of the TN inputs from the 1910s to the 1960s. Thereafter, the proportion of N  
 280 fertilizer substantially increased from 15% in the 1960s to 39 % in the 2010s, when manure N and  
 281 atmospheric N deposition accounted for 37% and 24% of N inputs, respectively.

282 Table 2. Decadal average of N inputs into the terrestrial ecosystem (Tg N yr<sup>-1</sup>)

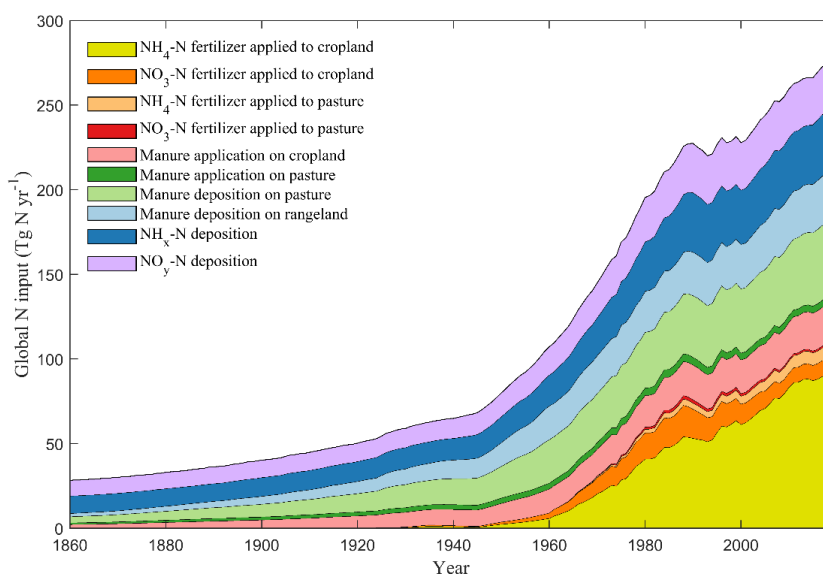
Decade	Nfer NH <sub>4</sub> Crop	Nfer NO <sub>3</sub> Crop	Nfer NH <sub>4</sub> Pas	Nfer NO <sub>3</sub> Pas	Nman App Crop	Nman App Pas	Nman Dep Pas	Nman Dep Ran	Ndep NH <sub>x</sub>	Ndep NO <sub>y</sub>	Total
1860s	0.00	0.00	0.00	0.00	2.52	1.01	3.92	2.04	10.32	9.24	29.05
1910s	0.08	0.05	0.00	0.00	6.54	2.20	9.87	6.38	11.59	10.72	47.43
1960s	11.81	5.98	0.19	0.12	14.86	3.60	26.99	20.77	20.15	18.35	122.80
1970s	28.21	12.09	1.21	0.72	17.23	4.14	30.77	23.17	25.40	22.98	165.94
1980s	47.27	16.98	2.97	1.67	19.46	4.54	34.22	24.49	31.90	27.34	210.83



1990s	56.42	14.59	4.02	1.73	20.19	4.29	36.99	25.67	33.80	28.55	226.26
2000s	70.32	10.57	5.77	1.33	20.66	4.01	39.57	27.50	33.45	28.73	241.91
2010s	87.52	9.03	7.39	1.10	22.29	4.09	43.25	28.68	35.58	28.30	267.23

283 Note: Nfer—N fertilizer, Nman—manure N, Ndep—N deposition, Crop—Cropland,  
 284 Pas—Pasture, Ran—Rangeland, App—Application, Dep—Deposition.

285



286

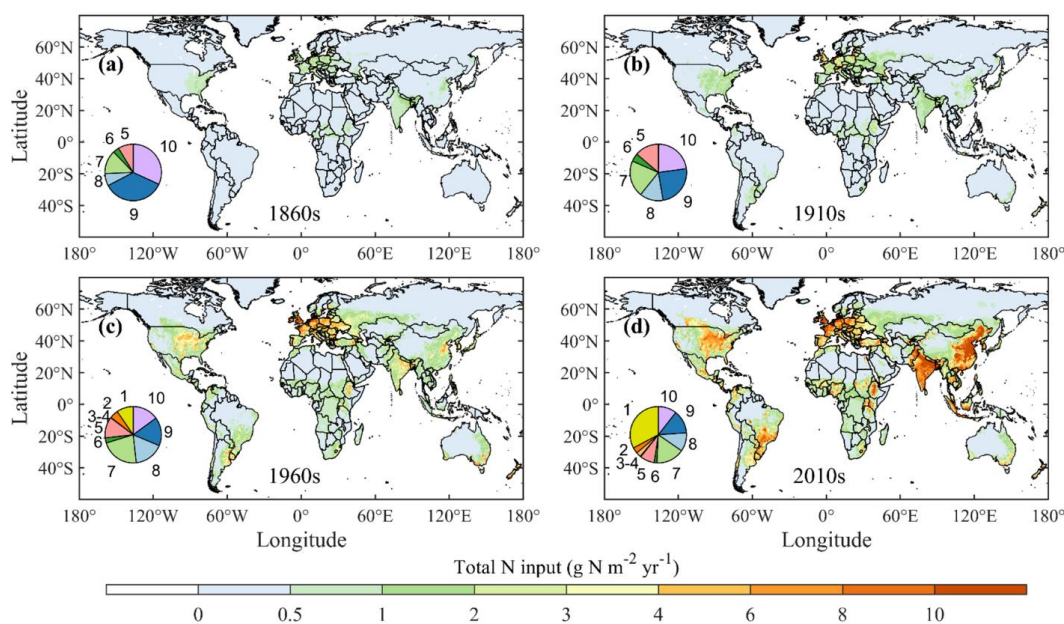
287 **Figure 4.** Long-term trends of anthropogenic nitrogen inputs to terrestrial ecosystems during 1860-  
 288 2019. N input to global terrestrial ecosystems from three major categories: N fertilizer, manure N,  
 289 and N deposition, which are further divided into ten specific types, including NH<sub>4</sub>-N fertilizer  
 290 applied to cropland, NO<sub>3</sub>-N fertilizer applied to cropland, NH<sub>4</sub>-N fertilizer applied to pasture, NO<sub>3</sub>-  
 291 N fertilizer applied to pasture, manure N application on cropland, manure N application on pasture,  
 292 manure N deposition on pasture, manure N deposition on rangeland, NH<sub>x</sub>-N deposition, and NO<sub>y</sub>-  
 293 N deposition.

294

295 The TN inputs exhibited high spatial heterogeneity across the globe, associated with the  
 296 imbalances in regional economic development and population growth (Fig. 5). From the 1860s to  
 297 the 1910s, the TN inputs mainly increased in the eastern U.S., Europe, and India, driven by the  
 298 increase in manure N application and deposition. In the 1960s, several hotspots of the TN inputs  
 299 emerged in Europe (Fig. 5c) where synthetic fertilizer was first widely used. Meanwhile, the TN  
 300 inputs were also intensified in many regions of the developing countries, such as eastern China,



301 southern Brazil, India, and countries in central Africa, mainly due to the increasing use of manure  
302 N (Fig. 5c). As the access to the synthetic N fertilizer became easier, the TN inputs significantly  
303 increased across the globe from the 1960s to the 2010s, and the inter-regional imbalance of N  
304 inputs had also been amplified, with regions of high N inputs concentrated in eastern and central  
305 China, India, Europe, midwestern U.S., and southern Brazil (Fig. 5d).



306

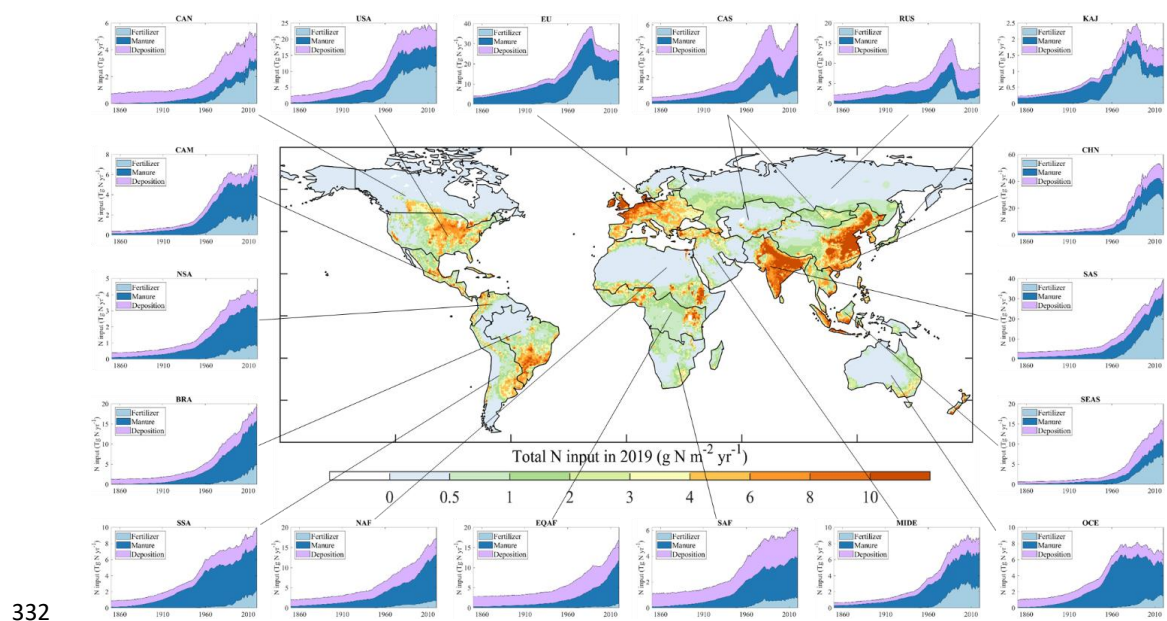
307 **Figure 5.** Spatial patterns of total N input in the (a) 1860s, (b) 1910s, (c) 1960s, and (d) 2010s.  
308 For the pie chart in the spatial map, the numbers 1-10 represent the percentage of each component,  
309 respectively (1. 'NH<sub>4</sub>-N fertilizer applied to cropland', 2. 'NO<sub>3</sub>-N fertilizer applied to cropland',  
310 3. 'NH<sub>4</sub>-N fertilizer applied to pasture', 4. 'NO<sub>3</sub>-N fertilizer applied to pasture', 5. 'Manure  
311 application on cropland', 6. 'Manure application on pasture', 7. 'Manure deposition on pasture',  
312 8. 'Manure deposition on rangeland', 9. 'NH<sub>x</sub>-N deposition', 10. 'NO<sub>y</sub>-N deposition').

313

314 Among the 18 regions (Fig 6), the top three regions with the highest TN inputs in 1960 were  
315 Europe (19.0 Tg N yr<sup>-1</sup>), USA (11.8 Tg N yr<sup>-1</sup>), and South Asia (9.9 Tg N yr<sup>-1</sup>). From 1960 to 2019,  
316 the largest increases in TN inputs were found in China, South Asia, and Brazil, which accounted  
317 for 26%, 18%, and 9% of the increase of the global N inputs, respectively. The increasing TN  
318 inputs in China and South Asia were mainly driven by the wide use of synthetic fertilizer, while  
319 those in Brazil were driven by the use of both livestock manure and synthetic fertilizer. The TN



320 inputs in USA became relatively stable since 1980, whereas the TN inputs in Europe decreased by  
 321 32% from 1988 to 2019, primarily due to the increase in crop N use efficiency and the reduction  
 322 in synthetic fertilizer application. Although the TN inputs in China experienced a rapid increase in  
 323 recent decades, it started to show a decreasing trend after 2014. However, the TN inputs in South  
 324 Asia and Brazil continued maintaining a strong growth trend. In 2019, China (49.1 Tg N yr<sup>-1</sup>)  
 325 contributed the largest share (18%) to global TN inputs, followed by South Asia (38.9 Tg N yr<sup>-1</sup>,  
 326 14%) and Europe (26.2 Tg N yr<sup>-1</sup>, 10%). The TN inputs in North America (USA and CAN), Europe  
 327 (EU), East and South Asia (CHN, KAJ, SAS, and SFAS) were dominated by synthetic fertilizer,  
 328 while those in Central and South America (BRA, SSA, NSA, and CAM), Africa (NAF, EQAF,  
 329 and SAF), Central and West Asia (CAS and MIDE), and Oceania (OCE) were dominated by manure.  
 330 RUS was the only region where atmospheric N deposition was the major anthropogenic  
 331 N source in 2019.



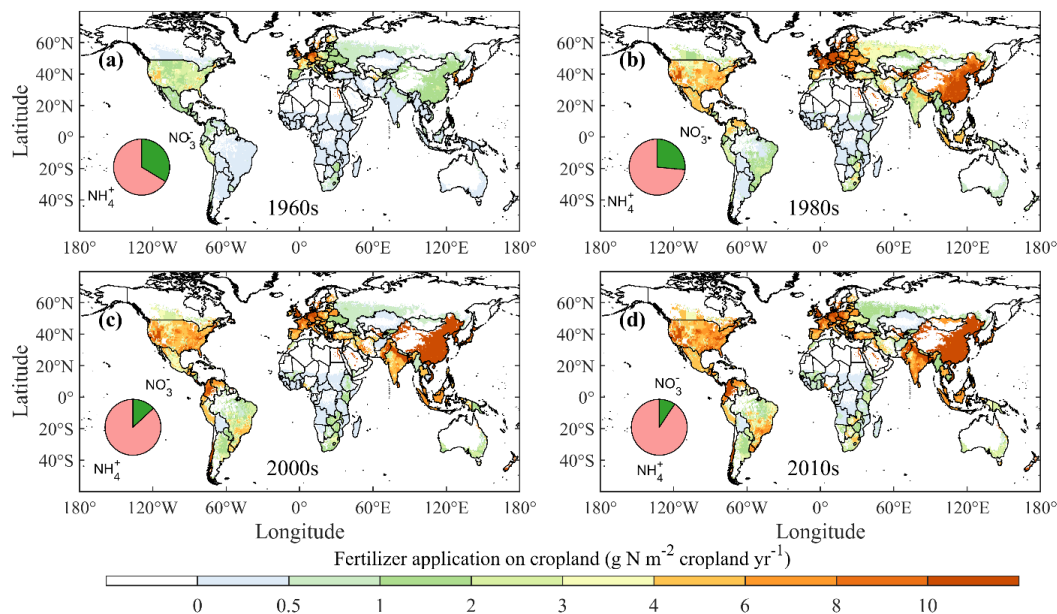
332  
 333 **Figure 6.** Long-term trends and variations of regional N inputs (synthetic fertilizer, livestock  
 334 manure, and atmospheric deposition) to terrestrial ecosystems during 1860-2019. The 18 regions  
 335 are USA, Canada (CAN), Central America (CAM), Northern South America (NSA), Brazil (BRA),  
 336 Southwest South America (SSA), Europe (EU), Northern Africa (NAF), Equatorial Africa (EQAF),  
 337 Southern Africa (SAF), Russia (RUS), Central Asia (CAS), Middle East (MIDE), China (CHN),  
 338 Korea and Japan (KAJ), South Asia (SAS), Southeast Asia (SEAS), and Oceania (OCE).



339

### 340 3.2. N fertilizer inputs on cropland and pasture

341 From the 1960s to the 2010s, the N fertilizer inputs on cropland and pasture increased from 18.1  
342 Tg N yr<sup>-1</sup> to 105.0 Tg N yr<sup>-1</sup>. Specifically, N fertilizer inputs on cropland increased from 17.8 Tg  
343 N yr<sup>-1</sup> to 96.6 Tg N yr<sup>-1</sup>, and N fertilizer inputs on pasture increased from 0.3 Tg N yr<sup>-1</sup> to 8.5 Tg  
344 N yr<sup>-1</sup> (Fig. 4 and Table 1). The proportion of NH<sub>4</sub><sup>+</sup> fertilizer in N fertilizer increased from 64%  
345 in the 1960s to 90% in the 2010s, contrarily NO<sub>3</sub><sup>-</sup>-N fertilizer decreased from 36% in the 1960s  
346 to 10% in the 2010s. At the regional level, Europe and USA were the top two N fertilizer-  
347 consuming regions in the 1960s, accounting for 38% and 25% of global N fertilizer application,  
348 while China (28%) and South Asia (21%) were the top two in the 2010s (Fig. 6). Fertilizer  
349 application rates in China and South Asia increased at a rate of 0.59 Tg N yr<sup>-2</sup> and 0.43 Tg N yr<sup>-2</sup>  
350 (p<0.05) during 1960-2019, respectively.



351

352 **Figure 7.** Spatial patterns of N fertilizer application on cropland in the 1960s, 1980s, 2000s, and  
353 2010s.

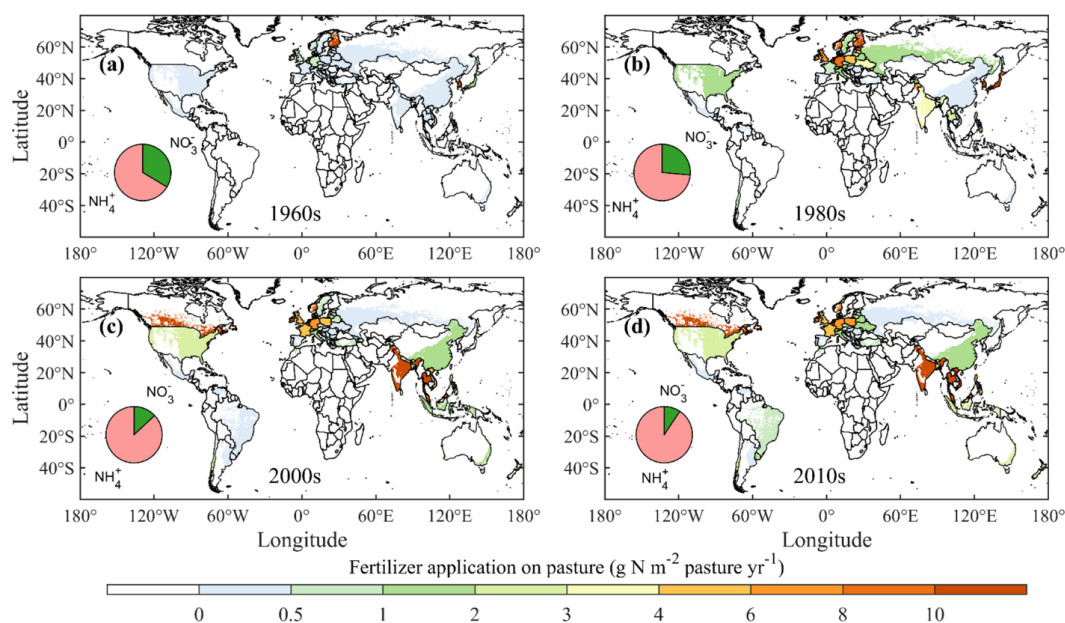
354

355 Fertilizer application rates on cropland in Europe reached the maximum in the 1980s, but fertilizer  
356 application rates in India, eastern Asia, and southern Brazil kept increasing continuously (Fig 7).



357 In the 2010s, extremely high N fertilizer inputs ( $> 20.0 \text{ g N m}^{-2} \text{ yr}^{-1}$ ) mainly occurred in eastern  
358 and southeastern China. Croplands in northern India and western Europe also had high N fertilizer  
359 rates ( $> 10.0 \text{ g N m}^{-2} \text{ yr}^{-1}$ ). N fertilizer application changed slowly in Africa, with most croplands  
360 receiving N fertilizer less than  $2.0 \text{ g N m}^{-2} \text{ yr}^{-1}$ . For pasture, Europe was the main region with N  
361 fertilizer application over  $6.0 \text{ g N m}^{-2} \text{ yr}^{-1}$  before the 1980s (Fig 8). N fertilizer application on  
362 pasture in southern Canada and India increased significantly with rates over  $8.0 \text{ g N m}^{-2} \text{ yr}^{-1}$  in the  
363 2010s. Most other regions (e.g., China, U.S. Brazil, Africa) received N fertilizer application of less  
364 than  $3.0 \text{ g N m}^{-2} \text{ yr}^{-1}$ .

365



366

367 **Figure 8.** Spatial patterns of N fertilizer application on pasture in the 1960s, 1980s, 2000s, and  
368 2010s.

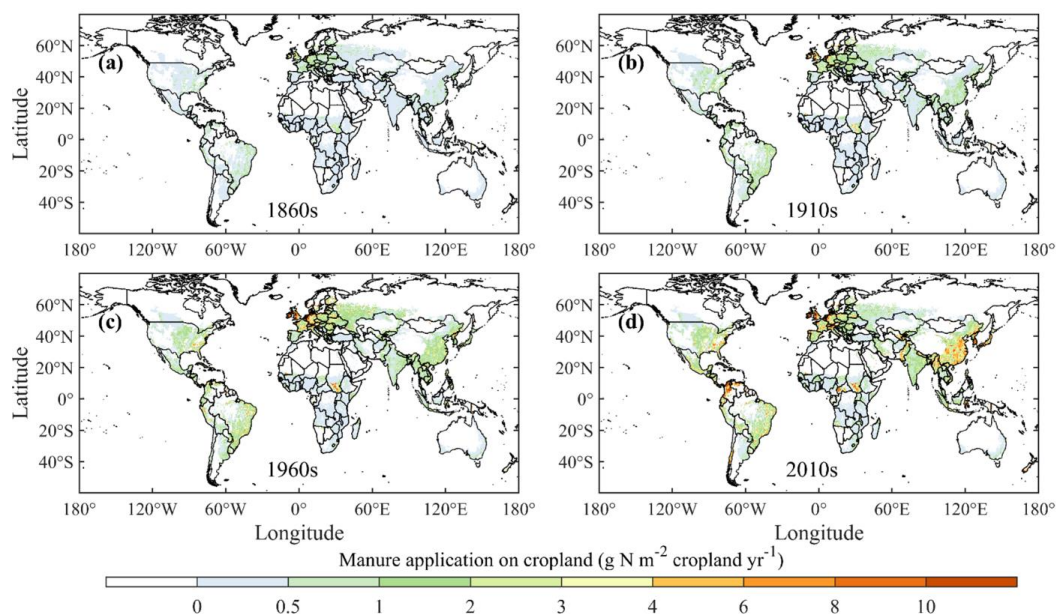
369

### 370 3.3. Manure N inputs on cropland, pasture, and rangeland

371 The total manure N inputs to land increased from  $9.48 \text{ Tg N yr}^{-1}$  in the 1860s to  $98.31 \text{ Tg N yr}^{-1}$  in  
372 the 2010s, with an increasing rate of  $0.6 \text{ Tg N yr}^{-2}$  (Fig 4 and Table 1). The manure N application  
373 on cropland, manure application on pasture, manure deposition on pasture, and manure deposition  
374 on rangeland changed from  $14.86 \text{ Tg N yr}^{-1}$  (22% of total manure input),  $3.60 \text{ Tg N yr}^{-1}$  (5%),



375 26.99 Tg N yr<sup>-1</sup> (41%), and 20.77 Tg N yr<sup>-1</sup> (31%) in the 1960s to 22.29 Tg N yr<sup>-1</sup> (23%), 4.09 Tg N yr<sup>-1</sup> (4%),  
376 N yr<sup>-1</sup> (4%), 43.25 Tg N yr<sup>-1</sup> (44%), and 28.68 Tg N yr<sup>-1</sup> (29%) in the 2010s, respectively. Europe  
377 was the largest contributor (39%) to global manure N inputs in the 1860s, but its share decreased  
378 in the last century and became 9% in the 2010s (Fig. 6). The manure N inputs in Brazil grew  
379 rapidly from 0.55 Tg N yr<sup>-1</sup> (2% of global manure N inputs) in the 1910s to 10.77 Tg N yr<sup>-1</sup> (11%)  
380 in the 2010s. Similarly, manure N inputs in Equatorial Africa and Northern Africa were only 2.22  
381 Tg N yr<sup>-1</sup> (3%) and 4.20 Tg N yr<sup>-1</sup> (6%) in the 1960s and increased dramatically to 9.40 Tg N yr<sup>-1</sup>  
382 (10%) and 10.60 Tg N yr<sup>-1</sup> (11%) in the 2010s, respectively. China was the largest contributor  
383 (12%) of global total manure N inputs in the 2010s, while it contributed 8% in the 1960s and 12%  
384 in the 1860s.



385

386 **Figure 9.** Spatial patterns of manure N application on cropland in the 1860s, 1910s, 1960s, and  
387 2010s.

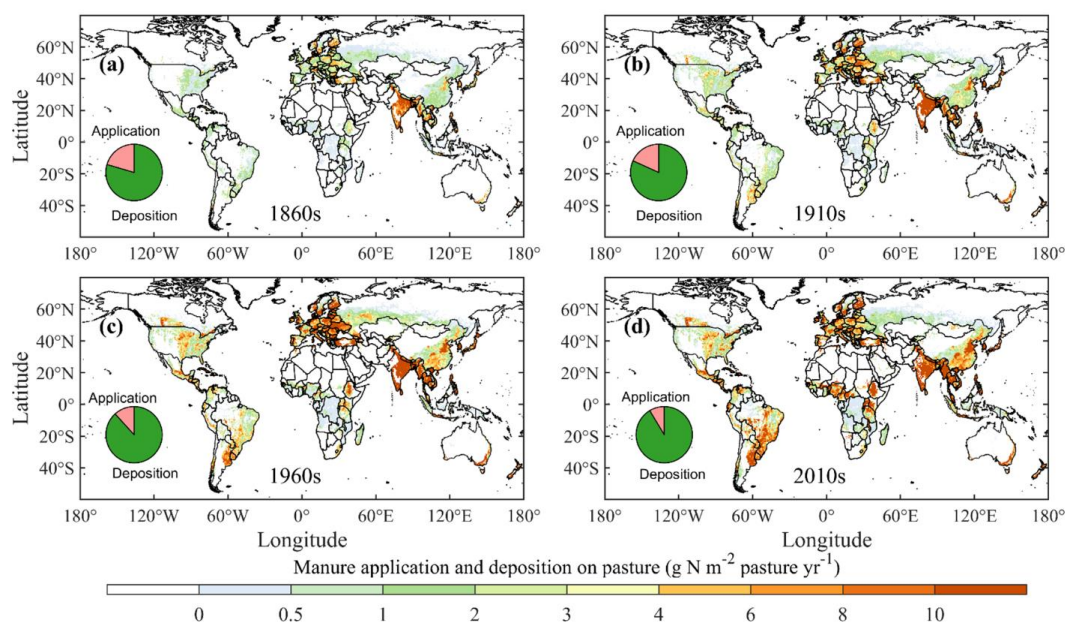
388

389 Manure application rates on cropland gradually intensified across the globe since the 1860s except  
390 in Australia and part of Africa (Fig. 9). Hotspots of manure application on cropland (> 6.0 g N m<sup>-2</sup>  
391 yr<sup>-1</sup>) first appeared in western Europe in the 1910s, then intensified manure application was  
392 observed in eastern Asia and northern South America in the 2010s. Manure application and



393 deposition on pasture had higher spatial variability than that on cropland (Fig. 10). Pasture in  
394 Europe and South Asia received higher manure N than that in other regions. Eastern South America,  
395 central Africa, and eastern Asia also experienced a significant increase in manure N inputs on  
396 pasture since the 1910s. For manure deposition on rangeland, South Asia stood out over the study  
397 period, with several other hotspots emerging in central Africa, northern China, Europe, and eastern  
398 South America since the 1910s (Fig 11).

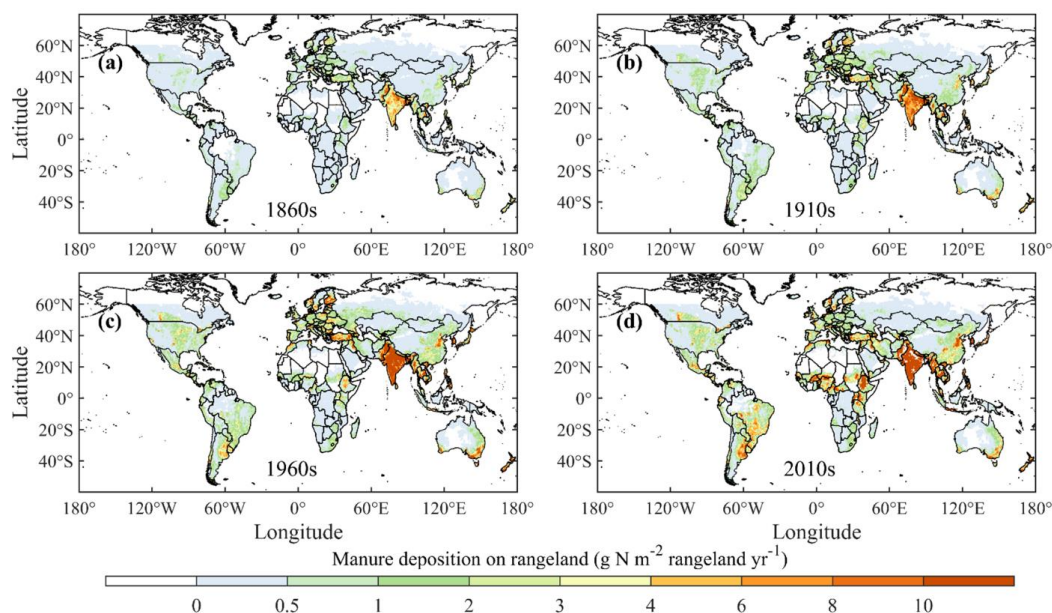
399



400

401 **Figure 10.** Spatial patterns of manure N application and deposition on pasture in the 1860s,  
402 1910s, 1960s, and 2010s.

403

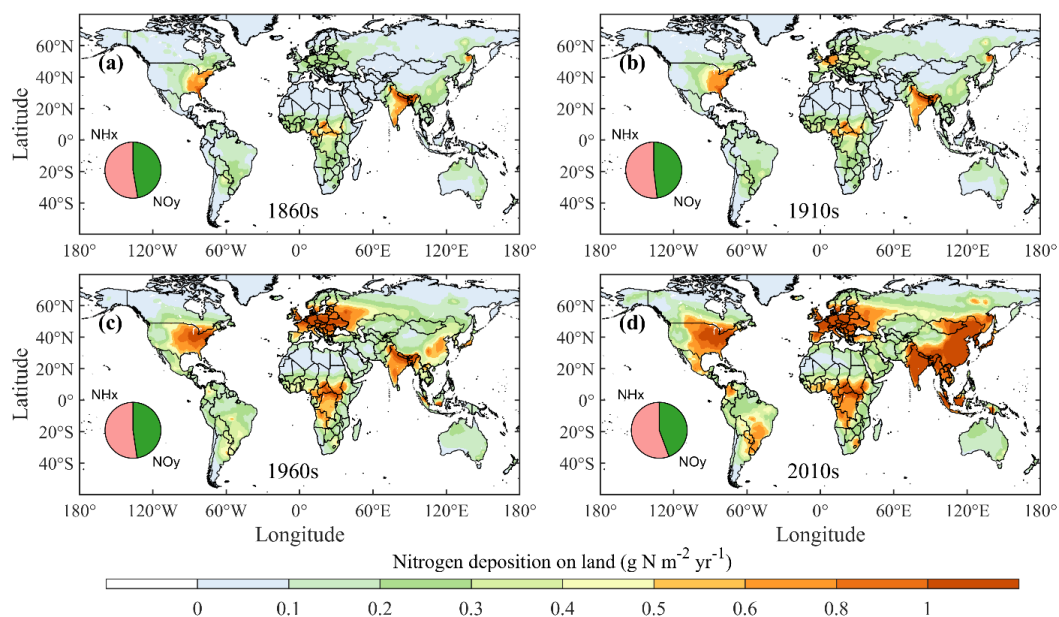


404

405 **Figure 11.** Spatial patterns of manure N deposition on rangeland in the 1860s, 1910s, 1960s, and  
406 2010s.

### 407 3.4. Atmospheric N deposition on land

408 Atmospheric N deposition has a threefold increase from 19.06 Tg N yr<sup>-1</sup> to 60.87 Tg N yr<sup>-1</sup> during  
409 the 1850s - the 2010s, with NH<sub>x</sub> deposition increasing from 10.02 Tg N yr<sup>-1</sup> to 35.58 Tg N yr<sup>-1</sup> and  
410 NO<sub>y</sub> deposition increasing from 9.04 Tg N yr<sup>-1</sup> to 28.30 Tg N yr<sup>-1</sup> (Fig 4 and Table 1). The share  
411 of NH<sub>x</sub> in atmospheric N deposition started to increase after the 1970s, changing from 52% to 56%  
412 in the 2010s. At the regional scale, South Asia, Equatorial Africa, and USA were the largest  
413 contributors in the 1860s, accounting for 13%, 13%, and 12% of global atmospheric N deposition,  
414 respectively (Fig 6). In the 2010s, China was the region with the largest atmospheric N deposition  
415 (10.66 Tg N yr<sup>-1</sup>, 17% of global atmospheric N deposition), followed by South Asia (5.90 Tg N  
416 yr<sup>-1</sup>, 9%) and USA (5.69 Tg N yr<sup>-1</sup>, 9%). Atmospheric N deposition peaked in the 1980s in Europe  
417 and Equatorial Africa, the 1990s in USA, and the 2010s in South Asia and China. Spatially,  
418 atmospheric N deposition intensified and increased dramatically across the globe since the 1910s  
419 (Fig. 12), and regions with high N deposition rates (>1.0 g N m<sup>-2</sup> yr<sup>-1</sup>) were mainly in Europe,  
420 central Africa, southern Asia, U.S. (since the 1960s), and eastern Asia (in the 2010s).



421

422 **Figure 12.** Spatial patterns of atmospheric N deposition on land in the 1860s, 1910s, 1960s, and  
423 2010s.

424

#### 425 **4. Discussion**

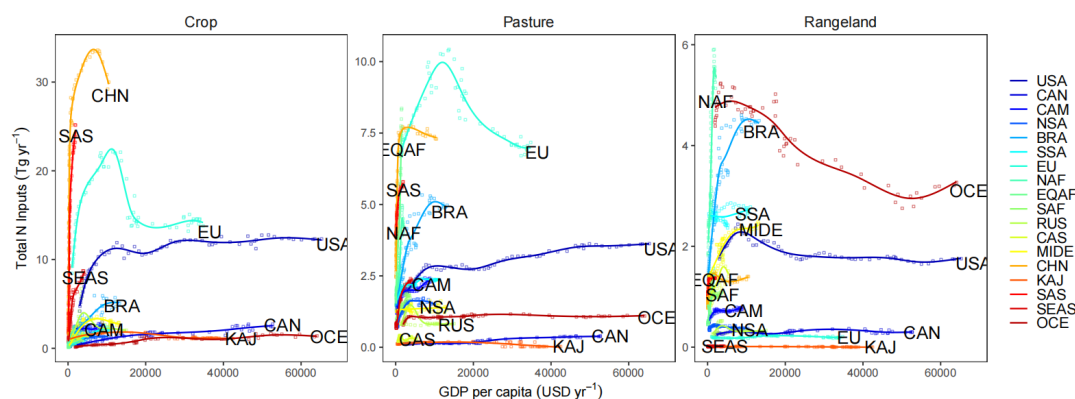
##### 426 **4.1 Socioeconomic forcing of N use**

427 The total anthropogenic nitrogen inputs (excluding N deposition) showed a close relationship with  
428 GDP per capita in all the three agricultural sectors of cropland, pasture, and rangeland (Fig. 13).  
429 These relationships could be generally categorized into three groups: a hump-shaped curve, a rapid  
430 increase curve, and an asymptote curve. The first was typically seen in regions like China and  
431 Europe. China, as the top N consumer, has successfully reduced its nitrogen use for crop  
432 production from the peak of 33.6 Tg yr<sup>-1</sup> in 2014 to 30.0 Tg yr<sup>-1</sup> in 2020. Crop production in China  
433 increased in the same period due to the improvements in crop varieties, fertilizer management, and  
434 land use policies (Cui et al., 2018; Wu et al., 2018). The mandatory policies and directives for N  
435 use in Europe since the late 1980s have effectively curbed its N use to a stable level (Van Grinsven  
436 et al., 2014). The second could be seen in South Asia, Southeast Asia, North Africa, etc. These  
437 regions are still in the developing stage and need to tackle the food demand of rapidly growing  
438 population, which, together with low nitrogen use efficiency, results in a surge of nitrogen



439 pollution (Chang et al., 2021). The third could be well represented by USA and Canada. For the  
440 USA, although its crop nitrogen use efficiency has considerably improved since the 1990s driven  
441 by technological and management improvements (Zhang et al., 2015), its cropland area has kept  
442 expanding recently with the new cropland usually producing yields below the national average  
443 (Lark et al., 2020), which undermines its efforts for reducing N excess induced environmental  
444 pollution. For the same curve type, there also existed obvious differences. For example, the turning  
445 points for crop N inputs in Europe and China emerged at varied socioeconomic development levels.  
446 Meanwhile, it was difficult to predict when China's crop N inputs would decrease to its lowest as  
447 Europe's case had shown. For different sectors of one country or region, their N inputs could also  
448 show asynchrony with GDP per capita increases. Take the USA as an instance, its N inputs on  
449 cropland and pasture kept growing while its N inputs on rangeland had kept stable. Despite such a  
450 diversity of the N use changes in varied socioeconomic circumstances, the N use-GDP per capita  
451 relationships and the related spatial patterns will be a valuable reference for any future projection  
452 of global anthropogenic N inputs.

453



454

455 **Figure 13.** Relationships between total N inputs (excluding N deposition) and GDP per capita in  
456 cropland, pasture and rangeland, respectively, within each of 18 regions during 1961-2019. The  
457 lines were fitted using the generalized additive models. For displaying clarity, not all region names  
458 are shown in each panel.

459

#### 460 4.2 Implications for nitrogen use management

461 Excessive N use has induced a variety of environmental issues, due to the magnitude, trend and  
462 the constitute forms. In regions or countries like Europe and the US, though the N inputs have been



463 stable (Fig. 13), the large magnitude of annual N inputs results in a considerable fraction of reactive  
464 N that is stored in soils. This N pool can cause strong legacy effects, of which the influence on  
465 water quality would last for decades (Meter et al., 2018). Therefore, maintaining the current levels  
466 of N inputs is far from reducing N related environmental issues in these regions or countries (Liu  
467 et al. 2016). Instead, agricultural nitrogen inputs are required to be eliminated drastically, which,  
468 however, seems rather difficult at the current technological level even the social-economic  
469 conditions are improving (Fig. 13). But for regions or countries like South Asia and Southeast Asia,  
470 where N inputs have been increasing rapidly, the management options or activities that are  
471 successful in Europe or USA can be promoted to inhibit the further increase of anthropogenic N  
472 inputs and local N induced pollution. This requires wide international collaboration and efficient  
473 coordination between developing countries and developed countries. As for the changes in N input  
474 forms, a signal worth noting is the increasing fraction  $\text{NH}_4^+$ -N in the global total N inputs (Figs. 7,  
475 8, and 12). High  $\text{NH}_4^+$ -N fraction has contributed significantly to N induced air pollution (Li et al.,  
476 2016), and the change of the ratio of  $\text{NH}_4^+$ -N over  $\text{NO}_3^-$ -N may affect biodiversity (van den Berg  
477 et al., 2016) and plant growth (Zhu et al., 2020; Yan et al., 2019). Improved use of  $\text{NH}_4^+$ -N will  
478 benefit both human society and ecosystems.

#### 479 **4.3 Limitations in data development and knowledge gaps**

480 The uncertainties and limitations of this global N input dataset are mainly derived from the  
481 following aspects: (1) Land use maps. Cropland, pasture, and rangeland distribution maps are  
482 critical for the spatialization of N fertilizer and manure application. In the data development  
483 process, we constrain N input amount of this dataset with the country-level fertilizer/manure  
484 consumption from FAO to ensure the total input consistent, but fertilizer use rate per unit cropland  
485 area could be significantly biased if the global data differs a lot from the country-specific data. For  
486 example, in the US, the higher cropland acreage in HYDE/LUH2 database, compared with the  
487 USDA census, is likely to make fertilizer input rate diluted, which could affect the impact  
488 assessment of N inputs (Yu and Lu, 2018). (2) Spatial patterns of fertilizer and manure application  
489 rate. The baseline of crop-specific fertilizer and manure use rates is fixed and has been used to  
490 determine the spatial patterns of fertilizer and manure inputs over the study period. This conflicts  
491 with the reality of inter-and intra-annual dynamics of crop rotation, annual changes in crop  
492 harvested area as well as changes in crop-specific fertilizer use rate over time. An ideal spatially  
493 explicit fertilizer input data, in the future, ought to consider the dynamics of crop rotation,



494 individual crop area changes, and crop-specific fertilizer use rate over space and time. (3) Country-  
495 level survey data. The country-level fertilizer and manure data from FAO don't separate N  
496 application to cropland and pasture. In this study, we separated fertilizer and manure application  
497 to cropland and pasture simply based on constant ratios generated by Lassaletta et al. (2014) and  
498 Zhang et al. (2015), which ignored either the temporal or the spatial changes of allocation of  
499 fertilizer and manure application to cropland and pasture. (4) Pre-1961 N inputs. Since the country-  
500 level fertilizer and manure data are only available after 1961, we assumed the change rates of  
501 global manure and fertilizer inputs before 1961 followed the change rates of annual global data  
502 reported by Holland et al. (2005). (5) Other N sources to terrestrial ecosystems. Leguminous green  
503 manure, which performs biological N fixation, was the most common nitrogen-containing soil  
504 fertility maintenance cropping practice before the widespread use of synthetic fertilizer, and is also  
505 used in current organic farming practices (Cherr et al., 2006). Since there are no statistics on the  
506 types and use of green manure on a global scale, it is necessary to develop a related database in  
507 future.

508 For future data improvements, we call for advanced N management survey/reporting mechanism  
509 to develop fine-scale N consumption or use rate data. For example, the commonly used survey  
510 data for the global fertilizer database is country-level consumption amount or crop-specific  
511 fertilizer input from IFA and FAO, which smoothed large variations in fertilizer application rate  
512 at farm level and sub-national scales. A continuous survey of crop-specific fertilizer and manure  
513 use at sub-national scale, development of dynamic global land use data, and crop rotation maps  
514 with more precise regional patterns are important for improving the resolution and accuracy of  
515 geospatial fertilizer and manure data. Additionally, considering fertilizer and manure application  
516 timing in the data is also important for agricultural nutrient management, which relies on the efforts  
517 and investigations regarding the fertilizer and manure application behavior at multiple spatial  
518 scales.

### 519 **Data availability**

520 The History of Anthropogenic N Inputs (HaNi) dataset is available at  
521 <https://doi.pangaea.de/10.1594/PANGAEA.942069> (Tian et al., 2022).



## 522 **Summary**

523 In this work, we developed a global annual anthropogenic N input dataset at 5-arcmin resolution  
524 during 1860-2019 by integrating multiple available databases into a uniform framework. This  
525 dataset for characterizing the History of anthropogenic N inputs (HaNi) includes major pathways  
526 and species of anthropogenic N input to the terrestrial biosphere, such as synthetic fertilizer N use  
527 in cropland and pasture, manure N application in cropland and pasture, manure N deposition in  
528 pasture and rangeland, and atmospheric N deposition. The TN input to global terrestrial  
529 ecosystems raised rapidly since the 1940s due to the widespread usage of synthetic N fertilizer,  
530 and the increase started to slow down after 2010. The hotspots of TN inputs shifted from Europe  
531 and North America to eastern and southern Asia. The TN inputs in North America, Europe, and  
532 East and South Asia were dominated by synthetic fertilizer, while those in Central and South  
533 America, Africa, Central, and West Asia, and Oceania were dominated by livestock manure. The  
534 N usage varied significantly in different socioeconomic circumstances, but the N use-GDP  
535 relationships still could provide a valuable reference for future projection of global anthropogenic  
536 N inputs. The HaNi dataset can serve as input data for a wide variety of modeling studies in earth  
537 system and its components (land, water, atmosphere and ocean), providing detailed information  
538 for the assessment of anthropogenic N enrichment impacts on global N cycling and cascading  
539 effects on climate, ecosystem, air and water quality. This data will keep updated in the future.

540

## 541 **Author contributions**

542 H.T. designed and led this work. Z.B., H.S. and X.Q. were responsible for developing the datasets.  
543 N.P. plotted all figures. F.N.T. and G.C. provided the FAO dataset. N.M. provided the crop-  
544 specific fertilizer and manure datasets. K.N. provided the fertilizer type dataset. S.P., C.L., and  
545 R.X. proposed the methods in the study. All authors contributed to the writing of the manuscript.

546

## 547 **Competing interests**

548 The authors declare that they have no conflict of interest.

549



550 **Acknowledgments**

551 This study has been partly supported by National Science Foundation (Grant numbers: 1903722;  
552 1922687), Andrew Carnegie fellowship Program (Grant No. G-F-19-56910). J.L. acknowledge  
553 National Natural Science Foundation of China (Grant no. 41625001), H.S. and X.Q. acknowledge  
554 National Key R & D Program of China (grant nos. 2017YFA0604702) and National Natural  
555 Science Foundation of China (Grant no. 41961124006). F.N.T. acknowledges funding from FAO  
556 regular programme. The views expressed in this publication are those of the author(s) and do not  
557 necessarily reflect the views or policies of FAO. K.N. is supported by a project, JPNP18016,  
558 commissioned by the New Energy and Industrial Technology Development Organization (NEDO)  
559 and a JSPS KAKENHI Grant Number JP18K11672. J.C. is supported by the Fundamental  
560 Research Funds for the Central Universities (2021QNA6005). We also thank James Gerber for  
561 providing us with the data on crop-specific nitrogen manure application.

562



## 563 References

- 564 Bargu, S., Justic, D., White, J. R., Lane, R., Day, J., Paerl, H., and Raynie, R.: Mississippi River  
565 diversions and phytoplankton dynamics in deltaic Gulf of Mexico estuaries: A review, *Estuar. Coast.*  
566 *Shelf Sci.*, 221, 39–52, <https://doi.org/10.1016/j.ecss.2019.02.020>, 2019.
- 567 van den Berg, L. J., Jones, L., Sheppard, L. J., Smart, S. M., Bobbink, R., Dise, N. B., and Ashmore, M.  
568 R.: Evidence for differential effects of reduced and oxidised nitrogen deposition on vegetation  
569 independent of nitrogen load, *Environ. Pollut.*, 208, 890–897, 2016.
- 570 Bian, Z., Tian, H., Yang, Q., Xu, R., Pan, S., and Zhang, B.: Production and application of manure  
571 nitrogen and phosphorus in the United States since 1860, *Earth Syst. Sci. Data*, 13, 515–527,  
572 <https://doi.org/10.5194/essd-13-515-2021>, 2021.
- 573 Bouwman, A., Dreht, G., and Van der Hoek, K.: Surface N balances and reactive N loss to the  
574 environment from global intensive agricultural production systems for the period 1970–2030, *Sci. China*  
575 *Ser. C Life Sci. Chin. Acad. Sci.*, 48 Suppl 2, 767–79, <https://doi.org/10.1007/BF03187117>, 2005.
- 576 Campbell, B. D. and Stafford Smith, D. M.: A synthesis of recent global change research on pasture and  
577 rangeland production: reduced uncertainties and their management implications, *Agric. Ecosyst. Environ.*,  
578 82, 39–55, [https://doi.org/10.1016/S0167-8809\(00\)00215-2](https://doi.org/10.1016/S0167-8809(00)00215-2), 2000.
- 579 Chang, J., Havlík, P., Leclère, D., de Vries, W., Valin, H., Deppermann, A., Hasegawa, T., and  
580 Obersteiner, M.: Reconciling regional nitrogen boundaries with global food security, *Nat. Food*, 2, 700–  
581 711, 2021.
- 582 Cherr, C. M., Scholberg, J. M. S., and McSorley, R.: Green manure approaches to crop production: A  
583 synthesis, *Agron. J.*, 98, 302–319, 2006.
- 584 Cui, X., Zhou, F., Ciais, P., Davidson, E. A., Tubiello, F. N., Niu, X., Ju, X., Canadell, J. G., Bouwman,  
585 A. F., Jackson, R. B., Mueller, N. D., Zheng, X., Kanter, D. R., Tian, H., Adalibieke, W., Bo, Y., Wang,  
586 Q., Zhan, X., and Zhu, D.: Global mapping of crop-specific emission factors highlights hotspots of  
587 nitrous oxide mitigation, *Nat. Food*, 2, 886–893, <https://doi.org/10.1038/s43016-021-00384-9>, 2021.
- 588 Cui, Z., Zhang, H., Chen, X., Zhang, C., Ma, W., Huang, C., Zhang, W., Mi, G., Miao, Y., and Li, X.:  
589 Pursuing sustainable productivity with millions of smallholder farmers, *Nature*, 555, 363–366, 2018.
- 590 Dodds, W. K.: Nutrients and the “dead zone”: the link between nutrient ratios and dissolved oxygen in the  
591 northern Gulf of Mexico, *Front. Ecol. Environ.*, 4, 211–217, [https://doi.org/10.1890/1540-9295\(2006\)004\[0211:NATDZT\]2.0.CO;2](https://doi.org/10.1890/1540-9295(2006)004[0211:NATDZT]2.0.CO;2), 2006.
- 593 Eickhout, B., Bouwman, A. F., and van Zeijts, H.: The role of nitrogen in world food production and  
594 environmental sustainability, *Agric. Ecosyst. Environ.*, 116, 4–14,  
595 <https://doi.org/10.1016/j.agee.2006.03.009>, 2006.
- 596 Eyring, V., Lamarque, J.-F., Hess, P., Arfeuille, F., Bowman, K., Chipperfield, M. P., Duncan, B., Fiore,  
597 A., Gettelman, A., and Giorgetta, M. A.: Overview of IGAC/SPARC Chemistry-Climate Model Initiative  
598 (CCMI) community simulations in support of upcoming ozone and climate assessments, *SPARC Newsl.*,  
599 40, 48–66, 2013.

600



- 601 Fowler D, Coyle M, Skiba U, Sutton MA, Cape JN, Reis S, Sheppard LJ, Jenkins A, Grizzetti B,  
602 Galloway JN, Vitousek P, Leach A, Bouwman AF, Butterbach-Bahl K, Dentener F, Stevenson D, Amann  
603 M, Voss M. The global nitrogen cycle in the twenty-first century. *Philos Trans R Soc Lond B Biol Sci*.  
604 368(1621):20130164, 2013. doi: 10.1098/rstb.2013.0164.
- 605 Friedlingstein, P., O'sullivan, M., Jones, M. W., Andrew, R. M., Hauck, J., Olsen, A., Peters, G. P.,  
606 Peters, W., Pongratz, J., and Sitch, S.: Global carbon budget 2020, *Earth Syst. Sci. Data*, 12, 3269–3340,  
607 2020.
- 608 Galloway, J. N., Aber, J. D., Erisman, J. W., Seitzinger, S. P., Howarth, R. W., Cowling, E. B., and  
609 Cosby, B. J.: The nitrogen cascade, *Bioscience*, 53, 341–356, 2003.
- 610 Galloway, J. N., Bleeker, A., and Erisman, J. W.: The Human Creation and Use of Reactive Nitrogen: A  
611 Global and Regional Perspective, *Annu. Rev. Environ. Resour.*, 46, 255–288,  
612 <https://doi.org/10.1146/annurev-environ-012420-045120>, 2021.
- 613 Gilbert, M., Nicolas, G., Cinardi, G., Van Boeckel, T. P., Vanwambeke, S. O., Wint, G. W., and  
614 Robinson, T. P.: Global distribution data for cattle, buffaloes, horses, sheep, goats, pigs, chickens and  
615 ducks in 2010, *Sci. Data*, 5, 1–11, 2018.
- 616 Gruber, N. and Galloway, J. N.: An Earth-system perspective of the global nitrogen cycle, *Nature*, 451,  
617 293–296, <https://doi.org/10.1038/nature06592>, 2008.
- 618 Holland, E. A., Lee-Taylor, J., Nevison, C., and Sulzman, J. M.: Global N Cycle: fluxes and N<sub>2</sub>O mixing  
619 ratios originating from human activity, ORNL DAAC, 2005.
- 620 Houlton, B. Z., Almaraz, M., Aneja, V., Austin, A. T., Bai, E., Cassman, K. G., Compton, J. E.,  
621 Davidson, E. A., Erisman, J. W., Galloway, J. N., Gu, B., Yao, G., Martinelli, L. A., Scow, K.,  
622 Schlesinger, W. H., Tomich, T. P., Wang, C., and Zhang, X.: A World of Cobenefits: Solving the Global  
623 Nitrogen Challenge, *Earths Future*, 7, 865–872, <https://doi.org/10.1029/2019EF001222>, 2019.
- 624 Howarth, R. W.: Coastal nitrogen pollution: A review of sources and trends globally and regionally,  
625 *Harmful Algae*, 8, 14–20, <https://doi.org/10.1016/j.hal.2008.08.015>, 2008.
- 626 Hurtt, G. C., Chini, L., Sahajpal, R., Frohling, S., Bodirsky, B. L., Calvin, K., Doelman, J. C., Fisk, J.,  
627 Fujimori, S., Klein Goldewijk, K., Hasegawa, T., Havlik, P., Heinemann, A., Humpeöder, F., Jungclaus,  
628 J., Kaplan, J. O., Kennedy, J., Krisztin, T., Lawrence, D., Lawrence, P., Ma, L., Mertz, O., Pongratz, J.,  
629 Popp, A., Poulter, B., Riahi, K., Shevliakova, E., Stehfest, E., Thornton, P., Tubiello, F. N., van Vuuren,  
630 D. P., and Zhang, X.: Harmonization of global land use change and management for the period 850–2100  
631 (LUH2) for CMIP6, *Geosci. Model Dev.*, 13, 5425–5464, <https://doi.org/10.5194/gmd-13-5425-2020>,  
632 2020.
- 633 Kanter, D., Winiwarter, W., Bodirsky, B., Bouwman, L., Boyer, L., Buckle, S., Compton, J., Dalgaard,  
634 T., de Vries, W., Leclère, D., Leip, A., Müller, C., Popp, A., Raghuram, N., Rao, S., Sutton, M., Tian, H.,  
635 Westhoek, H., Zhang, X., Zurek, M.: A framework for nitrogen futures in the shared socioeconomic  
636 pathways, *Global Environmental Change*, 61, 102029, 2020.  
637 <https://doi.org/10.1016/j.gloenvcha.2019.102029>.
- 638 Klein Goldewijk, K., Beusen, A., Doelman, J., and Stehfest, E.: Anthropogenic land use estimates for the  
639 Holocene – HYDE 3.2, *Earth Syst. Sci. Data*, 9, 927–953, <https://doi.org/10.5194/essd-9-927-2017>, 2017.



- 640 Lark, T. J., Spawn, S. A., Bougie, M., and Gibbs, H. K.: Cropland expansion in the United States  
641 produces marginal yields at high costs to wildlife, *Nat. Commun.*, 11, 1–11, 2020.
- 642 Lassaletta, L., Billen, G., Grizzetti, B., Anglade, J., and Garnier, J.: 50 year trends in nitrogen use  
643 efficiency of world cropping systems: the relationship between yield and nitrogen input to cropland,  
644 *Environ. Res. Lett.*, 9, 105011, <https://doi.org/10.1088/1748-9326/9/10/105011>, 2014.
- 645 Lassaletta, L., Billen, G., Garner, J., Bouwman, L., Velazquez, E., Mueller, N., Gerber, J.S.: Nitrogen use  
646 in the global food system: past trends and future trajectories of agronomic performance, pollution, trade,  
647 and dietary demand, *Environ. Res. Lett.*, 11 (2016), p. 095007, [10.1088/1748-9326/11/9/095007](https://doi.org/10.1088/1748-9326/11/9/095007).
- 648 Li, Y., Schichtel, B. A., Walker, J. T., Schwede, D. B., Chen, X., Lehmann, C. M., Puchalski, M. A., Gay,  
649 D. A., and Collett, J. L.: Increasing importance of deposition of reduced nitrogen in the United States,  
650 *Proc. Natl. Acad. Sci.*, 113, 5874–5879, 2016.
- 651 Liu, J., You, L., Amini, M., Obersteiner, M., Herrero, M., Zehnder, A. J. B., and Yang, H.: A high-  
652 resolution assessment on global nitrogen flows in cropland, *Proc. Natl. Acad. Sci.*, 107, 8035–8040,  
653 <https://doi.org/10.1073/pnas.0913658107>, 2010.
- 654 Liu, J., Ma, K., Ciais, P., and Polasky, S.: Reducing human nitrogen use for food production, *Sci. Rep.*, 6,  
655 30104, <https://doi.org/10.1038/srep30104>, 2016.
- 656 Lu, C. C. and Tian, H.: Global nitrogen and phosphorus fertilizer use for agriculture production in the past  
657 half century: shifted hot spots and nutrient imbalance, *Earth Syst. Sci. Data*, 9, 181, 2017.
- 658 Lun, F., Liu, J., Ciais, P., Nesme, T., Chang, J., Wang, R., Goll, D., Sardans, J., Peñuelas, J., and  
659 Obersteiner, M.: Global and regional phosphorus budgets in agricultural systems and their implications  
660 for phosphorus-use efficiency, *Earth Syst. Sci. Data*, 10, 1–18, <https://doi.org/10.5194/essd-10-1-2018>,  
661 2018.
- 662 Melillo, J. M.: Disruption of the global nitrogen cycle: A grand challenge for the twenty-first century,  
663 *Ambio*, 50, 759–763, <https://doi.org/10.1007/s13280-020-01429-2>, 2021.
- 664 Meter, K. J. V., Cappellen, P. V., and Basu, N. B.: Legacy nitrogen may prevent achievement of water  
665 quality goals in the Gulf of Mexico, *Science*, 360, 427–430, <https://doi.org/10.1126/science.aar4462>,  
666 2018.
- 667 Monfreda, C., Ramankutty, N., and Foley, J. A.: Farming the planet: 2. Geographic distribution of crop  
668 areas, yields, physiological types, and net primary production in the year 2000, *Glob. Biogeochem.*  
669 *Cycles*, 22, 2008.
- 670 Morgenstern, O., Hegglin, M. I., Rozanov, E., O'Connor, F. M., Abraham, N. L., Akiyoshi, H.,  
671 Archibald, A. T., Bekki, S., Butchart, N., and Chipperfield, M. P.: Review of the global models used  
672 within phase 1 of the Chemistry–Climate Model Initiative (CCMI), *Geosci. Model Dev.*, 10, 639–671,  
673 2017.
- 674 Mueller, N. D., Gerber, J. S., Johnston, M., Ray, D. K., Ramankutty, N., and Foley, J. A.: Closing yield  
675 gaps through nutrient and water management, *Nature*, 490, 254–257, <https://doi.org/10.1038/nature11420>,  
676 2012.



- 677 Nishina, K., Ito, A., Hanasaki, N., and Hayashi, S.: Reconstruction of spatially detailed global map of  
678  $\text{NH}_4^+$  and  $\text{NO}_3^-$  application in synthetic nitrogen fertilizer, *Earth Syst. Sci. Data*, 9, 149–162,  
679 <https://doi.org/10.5194/essd-9-149-2017>, 2017.
- 680 Pan, S., Bian, Z., Tian, H., Yao, Y., Najjar, R. G., Friedrichs, M. A. M., Hofmann, E. E., Xu, R., and  
681 Zhang, B.: Impacts of Multiple Environmental Changes on Long-Term Nitrogen Loading From the  
682 Chesapeake Bay Watershed, *J. Geophys. Res. Biogeosciences*, 126, e2020JG005826,  
683 <https://doi.org/10.1029/2020JG005826>, 2021.
- 684 Peñuelas, J. and Sardans, J.: The global nitrogen-phosphorus imbalance, *Science*, 375, 266–267,  
685 <https://doi.org/10.1126/science.abl4827>, 2022.
- 686 Potter, P., Ramankutty, N., Bennett, E. M., and Donner, S. D.: Characterizing the Spatial Patterns of  
687 Global Fertilizer Application and Manure Production, *Earth Interact.*, 14, 1–22,  
688 <https://doi.org/10.1175/2009EI288.1>, 2010.
- 689 Rabalais, N. N. and Turner, R. E.: Gulf of Mexico Hypoxia: Past, Present, and Future, *Limnol. Oceanogr.*  
690 *Bull.*, 28, 117–124, <https://doi.org/10.1002/lob.10351>, 2019.
- 691 Scheer, C., Pelster, D. E., and Butterbach-Bahl, K.: Editorial Overview: Climate change, reactive  
692 nitrogen, food security and sustainable agriculture-the case of  $\text{N}_2\text{O}$ , Elsevier, 2020.
- 693 Schlesinger, W. H. and Bernhardt, E. S.: Biogeochemistry: an analysis of global change, Academic press,  
694 2020.
- 695 Schlesinger, W. H., Reckhow, K. H., and Bernhardt, E. S.: Global change: The nitrogen cycle and rivers,  
696 *Water Resour. Res.*, 42, <https://doi.org/10.1029/2005WR004300>, 2006.
- 697 Stewart, W. M. and Roberts, T. L.: Food Security and the Role of Fertilizer in Supporting it, *Procedia*  
698 *Eng.*, 46, 76–82, <https://doi.org/10.1016/j.proeng.2012.09.448>, 2012.
- 699 Sutton, M. A., Bleeker, A., Howard, C. M., Erisman, J. W., Abrol, Y. P., Bekunda, M., Datta, A.,  
700 Davidson, E., De Vries, W., and Oenema, O.: Our nutrient world. The challenge to produce more food &  
701 energy with less pollution, Centre for Ecology & Hydrology, 2013.
- 702 Sutton MA, Howard CM, Kanter DR, Lassaletta L, Möring A, et al: The nitrogen decade: mobilizing  
703 global action on nitrogen to 2030 and beyond. *One Earth* 4:10–14, 2021.
- 704 Tian, H., Yang, J., Lu, C., Xu, R., Canadell, J. G., Jackson, R. B., Arneeth, A., Chang, J., Chen, G., Ciais,  
705 P., Gerber, S., Ito, A., Huang, Y., Joos, F., Lienert, S., Messina, P., Olin, S., Pan, S., Peng, C., Saikawa,  
706 E., Thompson, R. L., Vuichard, N., Winiwarter, W., Zaehle, S., Zhang, B., Zhang, K., and Zhu, Q.: The  
707 Global  $\text{N}_2\text{O}$  Model Intercomparison Project, *Bull. Am. Meteorol. Soc.*, 99, 1231–1251,  
708 <https://doi.org/10.1175/BAMS-D-17-0212.1>, 2018.
- 709 Tian, H., Yang, J., Xu, R., Lu, C., Canadell, J. G., Davidson, E. A., Jackson, R. B., Arneeth, A., Chang, J.,  
710 Ciais, P., Gerber, S., Ito, A., Joos, F., Lienert, S., Messina, P., Olin, S., Pan, S., Peng, C., Saikawa, E.,  
711 Thompson, R. L., Vuichard, N., Winiwarter, W., Zaehle, S., and Zhang, B.: Global soil nitrous oxide  
712 emissions since the preindustrial era estimated by an ensemble of terrestrial biosphere models:  
713 Magnitude, attribution, and uncertainty, *Glob. Change Biol.*, 25, 640–659,  
714 <https://doi.org/10.1111/gcb.14514>, 2019.



- 715 Tian, H., Xu, R., Canadell, J. G., Thompson, R. L., Winiwarter, W., Suntharalingam, P., Davidson, E. A.,  
716 Ciais, P., Jackson, R. B., Janssens-Maenhout, G., Prather, M. J., Regnier, P., Pan, N., Pan, S., Peters, G.  
717 P., Shi, H., Tubiello, F. N., Zaehle, S., Zhou, F., Arneth, A., Battaglia, G., Berthet, S., Bopp, L.,  
718 Bouwman, A. F., Buitenhuis, E. T., Chang, J., Chipperfield, M. P., Dangal, S. R. S., Dlugokencky, E.,  
719 Elkins, J. W., Eyre, B. D., Fu, B., Hall, B., Ito, A., Joos, F., Krummel, P. B., Landolfi, A., Laruelle, G. G.,  
720 Lauerwald, R., Li, W., Lienert, S., Maavara, T., MacLeod, M., Millet, D. B., Olin, S., Patra, P. K., Prinn,  
721 R. G., Raymond, P. A., Ruiz, D. J., van der Werf, G. R., Vuichard, N., Wang, J., Weiss, R. F., Wells, K.  
722 C., Wilson, C., Yang, J., and Yao, Y.: A comprehensive quantification of global nitrous oxide sources and  
723 sinks, *Nature*, 586, 248–256, <https://doi.org/10.1038/s41586-020-2780-0>, 2020a.
- 724 Tian, H., Xu, R., Pan, S., Yao, Y., Bian, Z., Cai, W.-J., Hopkinson, C. S., Justic, D., Lohrenz, S., Lu, C.,  
725 Ren, W., and Yang, J.: Long-Term Trajectory of Nitrogen Loading and Delivery From Mississippi River  
726 Basin to the Gulf of Mexico, *Glob. Biogeochem. Cycles*, 34, e2019GB006475,  
727 <https://doi.org/10.1029/2019GB006475>, 2020b.
- 728 Tian, H., Bian, Z., Shi, H., Qin, X., Pan, N., Lu, C., Pan, S., Tubiello, F. N., Chang, J., Conchedda, G.,  
729 Liu, J., Mueller, N., Nishina, K., Xu, R., Yang, J., You, L., and Zhang, B.: HaNi: a Historical dataset of  
730 Anthropogenic Nitrogen Inputs to the terrestrial biosphere (1860-2019),  
731 <https://doi.org/10.1594/PANGAEA.942069>, 2022.
- 732 Van Grinsven, H. J. M., Spiertz, J. H. J., Westhoek, H. J., Bouwman, A. F., and Erisman, J. W.: Nitrogen  
733 use and food production in European regions from a global perspective, *J. Agric. Sci.*, 152, 9–19, 2014.
- 734 Vitousek, P. M., Aber, J. D., Howarth, R. W., Likens, G. E., Matson, P. A., Schindler, D. W., Schlesinger,  
735 W. H., and Tilman, D. G.: Human Alteration of the Global Nitrogen Cycle: Sources and Consequences,  
736 *Ecol. Appl.*, 7, 737–750, [https://doi.org/10.1890/1051-0761\(1997\)007\[0737:HAOTGN\]2.0.CO;2](https://doi.org/10.1890/1051-0761(1997)007[0737:HAOTGN]2.0.CO;2), 1997.
- 737 Ward, B.: The Global Nitrogen Cycle, in: *Fundamentals of Geobiology*, edited by: Knoll, A. H., Canfield,  
738 D. E., and Konhauser, K. O., John Wiley & Sons, Ltd, Chichester, UK, 36–48,  
739 <https://doi.org/10.1002/9781118280874.ch4>, 2012.
- 740 West, P. C., Gerber, J. S., Engstrom, P. M., Mueller, N. D., Brauman, K. A., Carlson, K. M., Cassidy, E.  
741 S., Johnston, M., MacDonald, G. K., Ray, D. K., and Siebert, S.: Leverage points for improving global  
742 food security and the environment, *Science*, 345, 325–328, <https://doi.org/10.1126/science.1246067>,  
743 2014.
- 744 Wu, Y., Xi, X., Tang, X., Luo, D., Gu, B., Lam, S. K., Vitousek, P. M., and Chen, D.: Policy distortions,  
745 farm size, and the overuse of agricultural chemicals in China, *Proc. Natl. Acad. Sci.*, 115, 7010–7015,  
746 2018.
- 747 Xiong, Z. Q., Freney, J. R., Mosier, A. R., Zhu, Z. L., Lee, Y., and Yagi, K.: Impacts of population  
748 growth, changing food preferences and agricultural practices on the nitrogen cycle in East Asia, *Nutr.*  
749 *Cycl. Agroecosystems*, 80, 189–198, 2008.
- 750 Xu, R., Tian, H., Pan, S., Prior, S. A., Feng, Y., Batchelor, W. D., Chen, J., and Yang, J.: Global ammonia  
751 emissions from synthetic nitrogen fertilizer applications in agricultural systems: Empirical and process-  
752 based estimates and uncertainty, *Glob. Change Biol.*, 25, 314–326, <https://doi.org/10.1111/gcb.14499>,  
753 2019a.



- 754 Xu, R., Tian, H., Pan, S., Dangal, S. R. S., Chen, J., Chang, J., Lu, Y., Skiba, U. M., Tubiello, F. N., and  
755 Zhang, B.: Increased nitrogen enrichment and shifted patterns in the world's grassland: 1860–2016, *Earth*  
756 *Syst. Sci. Data*, 11, 175–187, <https://doi.org/10.5194/essd-11-175-2019>, 2019b.
- 757 Yan, L., Xu, X., and Xia, J.: Different impacts of external ammonium and nitrate addition on plant growth  
758 in terrestrial ecosystems: A meta-analysis, *Sci. Total Environ.*, 686, 1010–1018, 2019.
- 759 Yu, Z. and Lu, C.: Historical cropland expansion and abandonment in the continental U.S. during 1850 to  
760 2016, *Glob. Ecol. Biogeogr.*, 27, 322–333, <https://doi.org/10.1111/geb.12697>, 2018.
- 761 Zhang, B., Tian, H., Lu, C., Dangal, S. R. S., Yang, J., and Pan, S.: Global manure nitrogen production  
762 and application in cropland during 1860–2014: a 5 arcmin gridded global dataset for Earth system  
763 modeling, *Earth Syst. Sci. Data*, 9, 667–678, <https://doi.org/10.5194/essd-9-667-2017>, 2017.
- 764 Zhang, X., Davidson, E. A., Mauzerall, D. L., Searchinger, T. D., Dumas, P., and Shen, Y.: Managing  
765 nitrogen for sustainable development, *Nature*, 528, 51–59, <https://doi.org/10.1038/nature15743>, 2015.
- 766 Zhang, X., Zou, T., Lassaletta, L., Mueller, N. D., Tubiello, F. N., Lisk, M. D., Lu, C., Conant, R. T.,  
767 Dorich, C. D., Gerber, J., Tian, H., Bruulsema, T., Maaz, T. M., Nishina, K., Bodirsky, B. L., Popp, A.,  
768 Bouwman, L., Beusen, A., Chang, J., Havlík, P., Leclère, D., Canadell, J. G., Jackson, R. B., Heffer, P.,  
769 Wanner, N., Zhang, W., and Davidson, E. A.: Quantification of global and national nitrogen budgets for  
770 crop production, *Nat. Food*, 2, 529–540, <https://doi.org/10.1038/s43016-021-00318-5>, 2021.
- 771 Zhu, X., Yang, R., Han, Y., Hao, J., Liu, C., and Fan, S.: Effects of different NO<sub>3</sub><sup>-</sup>: NH<sub>4</sub><sup>+</sup> ratios on the  
772 photosynthesis and ultrastructure of lettuce seedlings, *Hortic. Environ. Biotechnol.*, 61, 459–472, 2020.

773